Journal of Morphology

# Comparative morphology of serotonergic-like immunoreactive elements in the Central Nervous System of kinorhynchs (Kinorhyncha, Cyclorhagida)

| | |
|---|---|
| Journal: | *Journal of Morphology* |
| Manuscript ID: | JMOR-12-0170.R2 |
| Wiley - Manuscript type: | Research Article |
| Date Submitted by the Author: | n/a |
| Complete List of Authors: | HERRANZ, MARIA; UCM, Zoology<br>Pardos, Fernando; UCM, Zoology<br>Boyle, Michael; Smithsonian Institution, |
| Keywords: | Kinorhyncha, nervous system, CLSM, serotonin, Cycloneuralia |
| | |

# Comparative morphology of serotonergic-like immunoreactive elements in the Central Nervous System of kinorhynchs (Kinorhyncha, Cyclorhagida)

María Herranz[1], Fernando Pardos[1] and Michael J. Boyle[2]

[1]*Dpto. Zoología y Antropología Física (Zoología de Invertebrados), Facultad de Biología, Universidad Complutense de Madrid, C/ José Antonio Novais, 2, 28040 Madrid, Spain.*

[2]*Smithsonian Marine Station at Fort Pierce. 701, Seaway Drive. Fort Pierce FL 34949 USA*

*E-mail:mariaherranz@bio.ucm.es. Tel.+34 91 394 49 55. Fax.91 394 49 47*



## ABSTRACT

Cycloneuralian taxa exhibit similar organ system architectures, providing informative characters of metazoan evolution, yet very few modern comparative descriptions of cellular and molecular homologies within and among those taxa are available. We immunolabeled and characterized elements of the serotonergic nervous system in the kinorhynchs *Echinoderes spinifurca*, *Antygomonas paulae* and *Zelinkaderes brightae* using confocal laser scanning microscopy. Fluorescent markers targeting DNA were combined with observations of auto-fluorescent structures to guide interpretations of the internal and external anatomy in each species. Results show a common pattern of the central nervous system with a circumenteric brain divided into ring-shaped anterior and posterior neuronal somata and a central neuropil connected to a multi-stringed, longitudinal ventral nerve cord. Structural similarities and differences in the nervous systems of these species were

observed and described, stressing the incomplete ring nature of the anterior region of the kinorhynch brain, the functional relationship between the brain and the movable introvert, and the number and arrangement of nerve strings and somata of the ventral nerve cord. The ventral cord ends in two ventrolateral cell bodies in *E. spinifurca*, and forms a terminal loop associated with a midterminal spine in *A. paulae* and *Z. brightae*. The possible functional and phylogenetic significance of these features and arrangements are discussed.

Key words: Kinorhyncha, nervous system, CLSM, serotonin, Cycloneuralia

## INTRODUCTION

Invertebrate nervous systems consist of complex, multifaceted sensory organs that typically represent distinct clade-specific cellular and molecular architectures (Bullock and Horridge, 1965; Schmidt-Rhaesa, 2007; Richter et al., 2010). Such distinction is exemplified by the Cycloneuralia (Ahlrichs, 1995; Introverta sensu Nielsen, 1995), a diverse invertebrate group that traditionally includes Nematomorpha, Nematoda, Priapulida, Kinorhyncha and Loricifera (Schmidt-Rhaesa et al., 1998; Nielsen, 2012; Schmidt-Rhaesa, 2007). Their name makes reference to an 'apomorphic' ring-like brain configuration; however, hypotheses vary as to whether cycloneuralians are considered a monophyletic group (Nielsen, 2001; Dunn et al., 2008; but see Hejnol et al. 2009) or represent a paraphyletic assemblage of taxa (Garey, 2001; Telford et al. 2008; Budd and Telford, 2009), and therefore the monophyletic status of Cycloneuralia is still open (Edgecombe et al. 2011).

Importantly, if it is possible that cycloneuralians gave rise to the arthropods (Budd and Telford, 2009), then modern comparative studies describing homologous organ systems between and within cycloneuralian taxa are both necessary, and appropriately aimed at revealing new insights into the evolution of Metazoa. Here, we describe cellular and molecular elements of the central nervous system in different kinorhynch species.

Kinorhyncha is a phylum of microscopic, segmented marine invertebrates that constitute part of the meiofauna. Due to their small size (less than 1mm in length) compound light microscopy does not provide enough resolution for describing their organ systems in detail. Previous studies focusing on their internal anatomy have been primarily based on transmission electron microscopy (TEM); e.g., (Brown, 1989; Gª Ordóñez et al., 2000; Kristensen and Hay-Schmidt, 1989; Kristensen and Higgins, 1991; Nebelsick, 1993; Neuhaus, 1994; Neuhaus and Higgins, 2002). Investigations on the structure of the nervous system in Kinorhyncha are scarce. To date, most of the studies on kinorhynchs described external features or ultrastructure of particular regions such as the introvert and mouth cone, or sensory organs. Studies are restricted to the genera *Echinoderes, Kinorhynchus* and *Pycnophyes*: *Echinoderes capitatus* Zelinka, 1928 (Nebelsick, 1991); *Kinorhynchus giganteus* Zelinka, 1928 *and Kinorhynchus phyllotropis,* Brown and Higgins, 1983 (Moritz and Storch, 1972 a, b; Brown, 1989) and *Pycnophyes greenlandicus* Higgins and Kristensen, 1988 (Kristensen and Higgins, 1991). The structure of the nervous system in kinorhynchs has been the subject of even fewer studies, or was part of a general anatomical overview typically dealing with no more than three species: *Echinoderes aquilonius* Higgins and Kristensen 1988; *P. greenlandicus* (Kristensen and Higgins, 1991); *E. capitatus* (Nebelsick, 1993); *Pycnophyes dentatus* Reinhardt, 1881, *Pycnophyes kielensis*

Zelinka, 1928 and *Zelinkaderes floridensis* Higgins, 1990 (Neuhaus, 1994). Most of these data have been reviewed in Neuhaus and Higgins (2002).

The kinorhynch nervous system is generally described as an orthogonal arrangement with several longitudinal nerve cords in the trunk that are connected by two commissures per segment (Zelinka, 1928; Kristensen and Higgins, 1991; Nebelsick, 1993; Neuhaus and Higgins, 2002). The brain is ring-like surrounding the anterior part of the gut and introvert retractor muscles. It is divided transversely into three regions consisting of anterior and posterior neuronal somata separated by a central neuropil. The anterior neuronal somata are organized into a ten-lobed structure with numerous perikarya forming a ventrally opened ring; the central region is a closed ring with a well-developed neuropil containing a comparatively low number of broadly distributed neuronal somata; the posterior neuronal somata contains numerous perikarya arranged in irregular accumulations (Kristensen and Higgins, 1991; Nebelsick, 1993; Neuhaus, 1994; Neuhaus and Higgins, 2002).

The combined use of histochemical or immunohistochemical methods and three-dimensional imaging by confocal laser scanning microscopy (CLSM) has become an important tool for describing complex organ systems in microscopic animals. Recently, detailed investigations have been performed for several interstitial invertebrate groups: Annelida (e.g. Worsaee and Rouse, 2010), Gastrotricha (e.g. Hochberg, 2007; Hochberg and Atherton, 2011), Mystacocarida (Brenneis and Richter, 2010), Rotifera (e.g. Hochberg and Gurbuz, 2008) and Priapulida (e.g. Rothe and Schmidt-Rhaesa, 2010) among others. However, thus far only three CLSM studies on Kinorhyncha have been reported: Rothe and Schmidt-Rhaesa (2002), Schmidt-Rhaesa and Rothe (2006) and Müller and Schmidt-Rhaesa (2003), which were focused on descriptions of the muscular system.

Animals use a wide variety of neurotransmitters in chemical synapses. No single transmitter type is used throughout the entire nervous system, thus it is not possible to characterize the whole nervous system using a single type of fluorescent marker (Rothe and Schmidt-Rhaesa, 2009). However, in order to establish a working protocol for labeling molecular components of the nervous system in kinorhynchs, it was reasonable to begin with standard markers such as antibodies against serotonin neurotransmitter molecules (5-HT; 5-Hydroxytryptamine, monoamine neurotransmitter). Our methods resulted in new data that enabled us to describe a subset of the nervous system. Due to the body wall structure of these animals having a resistant chitinous cuticle that prevents penetration of most chemical reagents such as antibodies, the application of immunohistochemical techniques with kinorhynchs represented a difficult challenge.

For this investigation we selected, examined and compared three cyclorhagid kinorhynchs species. We discuss our observations pertaining to several associated aspects of the central nervous system of kinorhynchs that may contribute to a broader understanding of evolution in Scalidophora and Cycloneuralia. This report is the first descriptive investigation of the nervous system in Kinorhyncha based on immunolabeling technology.

## MATERIALS AND METHODS

*Echinoderes spinifurca* Sørensen *et al.* 2005 and *Antygomonas paulae* Sørensen 2007 were collected in July and August 2011 from a series of designated sampling stations located offshore of the Fort Pierce Inlet, Florida, USA. The sampling stations were at intervals of nautical miles that included, 3 miles station– 27˚ 28.33' N, 80˚ 13.68' W; 4 miles station –

27° 28.19' N, 80° 12.76' W; 5 miles station – 27° 30.01' N, 80° 12.69' W; 6 miles station – 27° 29.18' N, 80° 10.98' W. Sampling depths ranged from 13–15 m among stations. *Zelinkaderes brightae* Sørensen 2007 was collected only from the first two stations.

Benthic marine sediment samples were collected from each station by deployment and retrieval of a Higgins anchor dredge (rectangular steel-box mouth opening: 29 cm width; 12.5 cm height) with a canvas collection bag (60 cm length). The dredge was attached to a 0.64 cm diameter cable that is connected to a hydrographic winch aboard the RV Sunburst, owned and operated by the Smithsonian Marine Station at Fort Pierce (SMSFP). Kinorhynchs were extracted from the sediment following the 'bubbling and blot' technique of Higgins (Higgins 1988; Sørensen and Pardos 2008). Live specimens were isolated, identified, and fixed with 4% paraformaldehyde (PFA) in filtered seawater (FSW) overnight at 4ºC. Following fixation, specimens were washed with multiple exchanges of phosphate buffered saline (PBS) and stored at 4ºC in a solution of PBS + 5.0 % sodium azide ($NaN_3$) to prevent microbial growth and contamination.

Scanning Electron Microscopy

For scanning electron microscopy (SEM), previously fixed specimens were dehydrated through a graded series of ethanol dilutions (10%-100%). Specimens in 100% ethanol were dried with $CO_2$ in a Tousimis Samdri-790 Critical Point Dryer (Tousimis Research Corp., Rockville, MD USA). The dried specimens were mounted on aluminum stubs, sputter coated with gold-palladium and imaged with a HITACHI S4800 field emission scanning electron microscope (Hitachi High-Technologies America, Inc., Pleasanton, CA USA);

coating and SEM imaging were performed at the United States Department of Agriculture (USDA), United States Horticultural Research Laboratory in Fort Pierce, Florida.

Propidium iodide labeling

Fixed specimens of each kinorhynch species were transferred from PBS into PBT (PBS + 2.0% Triton X-100), followed by several additional exchanges of PBT. Specimens were treated with RNase A at 1.0 mg/ml PBT for 1h at 37ºC to remove RNA molecules from cells. Animals were then treated with a fluorescent stain for nucleic acids, propidium iodide (PI), at 5.0 µg/ml PBT for a period of 48-72 hrs at 4ºC. When utilized as a singe molecular marker, or in combination with fluorescently conjugated antibodies, PI labeling was terminated with multiple exchanges of PBS prior to imaging by CLSM.

Immunohistochemistry

*Echinoderes spinifurca* (n= 20) was selected as the primary model in which to characterize the immunoreactivity of antibodies to serotonin (5-HT) neurotransmitter molecules. We also performed anti-5-HT treatments with specimens of *A. paulae* (n=5) and *Z. brightae* (n=3). The cuticle of *E. spinifurca* was permeablilized by the removal of terminal spines or penetration of the terminal segment by micro-dissection. Dissected animals were incubated in blocking solution (PBT + 0.5% bovine serum albumin (BSA) + 10% normal goat serum) at 4 ºC overnight. Specimens were incubated with a primary, rabbit anti-serotonin (5-HT) antibody (Sigma-Aldrich Inc.) at a concentration of 1:500 in blocking solution, at 4 ºC for 72 hrs. Primary anti-5-HT was removed with multiple exchanges of PBT. Specimens were then incubated with a secondary anti-rabbit $F(ab')_2$ fragment–Cy3 antibody (Sigma-Aldrich

Inc.) at a concentration of 1:500 in blocking solution, at 4 ºC for 72 hrs. Fresh preparations of primary and secondary antibodies were exchanged daily during each incubation, respectively. Secondary antibodies were removed with multiple exchanges of PBT, followed by three 15-minute exchanges of PBS prior to mounting. Incubations and fluid exchanges were performed in Pyrex spot plates, in the dark, while rocking.

Confocal laser scanning microscopy (CLSM)

Specimens labeled with PI or Cy3 secondary antibodies were attached to glass slides on a central mount of double-stick tape. Two strips of clear tape were placed on each side of the central mount to elevate the placement of a coverslip above the specimens. The slides were transferred through graded series of isopropanol dilutions, and then immersed and mounted in a 2:1 mixture of benzyl benzoate and benzyl alcohol. A coverslip was placed across the strips of clear tape and sealed with clear nail polish. Alternatively, specimens were immersed and mounted in glycerol (60% glycerol, 1x PBS) on glass slides with a coverslip elevated above the specimens by modeling clay. All labeled specimens were analyzed and imaged using a Zeiss LSM 510 confocal laser scanning microscope with Zen 2009 software (Carl Zeiss, Thornwood, NY) at the Smithsonian Marine Station at Fort Pierce. Optical sections and z-stack projection micrographs were compiled from LSM files with ImageJ, version 1.45m (Wayne Rasband, National Institutes of Health, USA). Original SEM and CLSM micrographs were edited with Adobe Photoshop CS4 (Adobe Systems Incorporated, San Jose, CA USA). Schematics and figure plates were prepared with Adobe Illustrator CS4 (Adobe Systems Incorporated, San Jose, CA USA).

Positional information used for describing external characters, internal anatomy, functional morphology and the associated molecular labeling of PI and 5-HT-like immunoreactivity follows the terminology and taxonomic standards for kinorhynchs as stated by Pardos et al. (1998), Neuhaus and Higgins (2002) and Sørensen and Pardos (2008); accordingly, trunk segments are numbered anterior to posterior from 1 to 11. Nervous system terminology follows the neuroanatomical glossary of Richter et al. (2010). The authors avoid using the terms forebrain, midbrain and hindbrain introduced by previous publications describing kinorhynch nervous systems, and instead, we use anterior neuronal somata, central neuropil and posterior neuronal somata, respectively.

The functional anatomy of the introvert in kinorhynchs, and other cycloneuralians, may complicate the interpretation of particular structures regarding their position in the trunk and their relationship with other organs. It is important to consider that anterior organs, such as the gut and brain, move when the introvert is extended or retracted. And variation in the response of specimens to chemical fixation makes it difficult to determine the precise degree of extension or retraction of the introvert at the moment of death. Consequently, the brain and associated structures of the nervous system may be observed in different positions. When the introvert is fully withdrawn, the brain may be located towards segment 3; however, when the introvert is totally extended, the anterior margin of the brain is situated just below the first scalid row. For additional clarification in this study, we use in the term *cord* when referring to the entire bundle of midventral, longitudinal neurites with more or less defined perykarial aggregations. Individual longitudinal ventral neurites that are shown with different arrangements in our images will be referred to as *strings*.

## RESULTS

*Echinoderes spinifurca*, *Antygomonas paulae* and *Zelinkaderes brightae* differ in their external morphology (Figs. 1, S-1), and internal anatomy. Microscope analyses and imaging of species-specific external and internal characters reveal several correlations with our results from molecular labeling experiments.

### Propidium iodide labeling

DNA labeling with propidium iodide shows a high concentration of cell nuclei surrounding the pharynx, which marks the location of the brain in all species under investigation (Figs. 2A, 3A, 4A). These cell nuclei are arranged in three distinct groups from anterior to posterior. In *E. spinifurca*, the first group exhibits a wide bilaterally symmetric, 10-lobed structure in association with the first ring of introvert scalids (spinoscalids). This structure has a gap in its midventral region (Fig. 2C-D), and represents the position of an aggregation of anterior neuronal somata. In *A. paulae,* the 10-lobed structure is less distinct with relatively large cell nuclei, and it forms a ring in the shape of a horseshoe that is midventrally opened (Fig. 3B-C).Specimens of *Z. brightae* could not be examined in orthogonal sections. The second group of nuclei corresponds with the position of the central neuropil and presents a comparatively lower concentration of nuclei in each of the three genera studied (Figs. 2A, E; 3A, C; 4A). In each species, the third group of nuclei contains a high concentration in several irregular lobes, and corresponds with the position of an aggregation of posterior neuronal somata (Figs. 2A; 3A, D; 4A).

There is a concentration of cell nuclei arranged longitudinally from anterior to posterior along the midventral line in the trunk segments of *E. spinifurca*, *A. paulae* and *Z. brightae*, which likely represent the ventral nerve cord (vnc). In *E. spinifurca*, longitudinal strands of nuclei diverge from the midline in segment nine, and exhibit an inverted Y-shaped pattern that terminates at ventrolateral positions in segment 10 (Fig. 4A). In contrast, *A. paulae* and *Z. brightae* show a loop of cell nuclei extending ventrally from segment 10 to segment 11 (not shown).

Anti-serotonin (5-HT) antibody labeling

Positive anti-serotonin-like immunoreactivity (IR) was detected for several elements of the central nervous system in *E. spinifurca* (Figs. 4, 5, 6, 7), *A. paulae* and *Z. brightae* (Figs. 8, 9). Permeabilization of the cuticle in *Z. brightae* was problematic for antibody penetration and therefore labeling was incomplete. Autofluorescence of the kinorhynch cuticle (Fig. S-1) as well as non-specific binding of secondary antibodies to the scalids and some portions of the epidermis also made overall signal detection difficult.

Fifteen out of twenty specimens of *E. spinifurca* showed positive staining with a common pattern of anti-5-HT-like IR characterized by several anterior nerve rings and a ventral longitudinal nerve cord (Figs. 4B, 5, 6). When the introvert is retracted, there are two serotonergic-positive rings that are each incomplete on their respective ventral sides, and they are situated between trunk segments 2 and 3; when the introvert is extended, these rings are positioned at the level of the second row of scalids (Figs. 6B-D, 7A). The first incomplete ring ($inr_1$) is shaped like a bracelet or necklace, which is ventrally opened and extends from two relatively large, distinct ventromedial somata (vms) showing high levels

of anti-5HT-like IR (Figs. 4B, 6, 7); possible additional somata could be associated with this ring. The second incomplete ring ($inr_2$) lacks distinct ventromedial somata and is adjacent to the first ring, and together they form a structural ring complex (rc) putatively assigned to the central neuropil, although large, conspicuous ventromedial somata appear to lie within the anterior neuronal somata. 5-HT-like labeling distinguishes these rings as individual units. The two rings are connected to a smaller ring, a mouth cone nerve ring (mcnr), which is fixed at the base of the mouth cone through fine neurites, and although weakly labeled, together they form a basket-like configuration characterized by these fine basket neurites (bne) and the nerve ring (Figs. 5, 6A, 7). In *E. spinifurca*, the basket-like structure is movable and always observed anterior to the two incomplete rings described above (Figs.4B, 5A, 6A, E, 7). However, when the introvert is retracted in *A. paulae* and *Z. brightae*, the smaller ring (mcnr) of the basket-like structure is positioned posteriorly in the trunk at the fifth segment level (Figs. 8A, 9A, 10A, B). The general appearance of the incomplete rings resembles a "string of pearls" that putatively contains a distribution of 5-HT-like IR synaptic vesicles along the ring-shaped neurites. An additional, complete double ring ($nr_{3,4}$) is situated posterior to, and parallel with, the incomplete rings mentioned above (Fig. 5A, 6B, E, 7, 10C). This double ring is weakly labeled and varies among individuals, but can be putatively assigned to the central neuropil. The entire ring complex (rc) (brain, mouth, and mouth cone nerve ring) may be altered in its location depending upon the position of the introvert. This is not the case for the ventral nerve cord, which is fixed to the trunk body wall (Figs. 6B-D, 7).

The second incomplete nerve ring ($inr_2$) is not continuous on its ventral side where it joins two convergent neurites (cne) midventrally at the transition between the brain and

ventral nerve cord (Figs. 4B, 5, 7). At this transition, each side of the ring extend parallel into a nerve cluster (nc) that joins with neurites of the ventral nerve cord on its posterior end. Movement of the ring complex during extension and retraction of the introvert determines the anterior-posterior position of the convergent neurites (Fig. 6B-D, 7). From this point, each of the two neurites branch to form a total of four strings for a short distance (Fig.5B). The two inner strings join to form a single central neurite that is flanked by two outer strings (Fig. 5B). This is the transition where the strings become attached to the body wall and maintain a fixed position independent of extension or retraction of the introvert (Fig. 5B, 6B-D).

This arrangement constitutes the ventral nerve cord extending along the trunk toward the posterior end of the animal (Figs. 5, 6, 7). It should also be noted here that ventral paired neuronal somata (vps) are segmentally arranged along the ventral cord in segments 1–9 and they are most distinct on the two lateral strings. The central string shows many regularly spaced somata, but they are not grouped in a segmental pattern (Figs. 5, 6B-D). Within segment 9, the midventral string terminates in a single cell body, while the two lateral strings continue posteriorly to segment 10 where they diverge and terminate in two ventrolateral somata (vls) that are relatively large and distinct (Figs. 4B, 5A, 6B-D). Anti-5-HT-like IR of transverse connections or commissures was not clearly detected between elements of the three ventral strings. We also did not detect neurites or anti-5-HT-like labeling of structures emerging from either caudal aggregations or somata of the ventral nerve cord. Similarly, no other longitudinal nerve strings or bundles were found. Nevertheless, positive anti-5HT-like IR exhibits intensity variation among specimens, so

we cannot exclude the possibility that other rings or bundles were overlooked or weakly stained.

Specimens of *A. paulae* and *Z. brightae* also show positive anti-5-HT-like IR with a similar overall pattern to *E. spinifurca* (Figs. 8A, 9A), although differences between the three species can be detected. *A. paulae* exhibits at least two additional pairs of midlateral somata (mls) connected to the incomplete anterior nerve rings through very fine neurites (Figs. 8A-B, 10B). Only one pair of such midlateral structures can be detected in *Z. brightae* (Figs. 9A, 10A). The ventral nerve cords in both *Z. brightae* and *A. paulae* are composed of four separate neurites containing abundant somata along the entire trunk length, although a paired arrangement of neuronal somata reflecting the morphology of segmental ganglia is not apparent (Figs. 8A-C, 9A-B). The two central neurites terminate in a single neural soma within segment 9, while lateral neurites extend posteriorly to two slightly divergent somata in segment 10. From these somata, a conspicuous circular neurite, or terminal neural loop (tl) occupies the posteriormost segment in specimens of those two species (Figs. 8C, 9A-B).

## DISCUSSION

### Brain

As reported by Kristensen and Higgins (1991) using transmission electron microscopy, the brain is divided from anterior to posterior into three ring-like regions. The anterior and posterior regions contain multiple neuronal cell bodies (perikarya), while the central neuropil contains fewer perikarya and more fibers when compared with the other two brain

regions (Kristensen and Higgins, 1991; Nebelsick, 1993; Neuhaus, 1994; Neuhaus and Higgins, 2002). Using DNA labeling, we found that patterns of cell nuclei in *E. spinifurca*, *A. paulae* and *Z. brightae* confirm the descriptions mentioned above. It was possible to identify a high concentration of neuronal cell bodies in the anterior part of the trunk surrounding the pharynx and to distinguish three ring-like aggregations of perikarya, showing that the anterior and posterior regions clearly contain more perikarya than the central neuropil. The ten-lobed division reported by Kristensen and Higgins (1991) for *Echinoderes aquilonius* is identifiable in *E. spinifurca*, most notably in the anterior neuronal somata. This division was not as distinct in *A. paulae*, and no transverse sections were characterized from specimens of *Z. brightae*. All species under investigation indicate the circumpharyngeal brain is not a completely closed ring, and reveals the appearance of a horseshoe-shaped pattern in the aggregations of anterior neuronal somata. This was previously reported for *E. capitatus* (Nebelsick, 1993).

The serotonin-like positive labeling shows a subset of the nervous system. The presence of four rings, two of them midventrally incomplete, located between segments two and three (with the introvert withdrawn) was consistent in all specimens of *E. spinifurca* with detectable labels. Very similar results were obtained with specimens of *A. paulae* and *Z. brightae*. Because it is hypothesized that serotonin is the primary myoexcitatory neurotransmitter in several invertebrate groups (Hochberg, 2009), it is reasonable to assume that the ring complex of kinorhynchs may be involved in locomotory processes. However, serotonin may also be activating 5-HT receptors on the membranes of different cell types within or outside of the central nervous system. Additional labeling in other potential cell types or associated organ systems containing 5-HT-like targets was not detected, or may

not be detectable, with the combination of primary anti-5-HT and secondary antibodies applied during this investigation.

Although kinorhynchs are known to have several neurites innervating the introvert scalids (Kristensen and Higgins, 1991; Nebelsick, 1993) we were not able to label any of them. A mechanoreceptor and chemoreceptor sensory function for introvert scalids has been advanced by Moritz and Storch (1972a, b) and Kristensen and Higgins (1991). The latter authors also suggest a locomotory function. However, no muscles appear to be directly associated with introvert scalids (Kristensen and Higgins, 1991; Müller and Schmidt-Rhaesa, 2003), and our results with serotonin-like labeling do not support a role in the direct motor control of scalids from the nervous system. Because it is clear that the introvert scalids contribute to forward movement of the animal, we conclude that the motion of scalids may be indirect, through contraction of dorsoventral muscles in the trunk that increase internal body pressure (Zelinka, 1928). We further hypothesize that stimulation for the muscular contraction of introvert retractors is accomplished by the ring complex and, especially, the ventromedial pair of neuronal cell somata.

In contrast to the introvert scalids, the nine oral styles of the mouth cone do possess muscles (Kristensen and Higgins, 1991; Nebelsick, 1993; Neuhaus, 1994). Accordingly, we find an anti-5HT-like immunoreactive nerve ring in the base of the mouth cone, which moves forward and backward with the protrusible mouth cone and is connected to the incomplete nerve rings by the "basket neurites" referred to above. It is remarkable that the functional differences between an eversible introvert and a protrusible mouth cone may be apparent in components of the nervous system controlling their movements.

Innervation of pharynx musculature could not be detected with anti-5-HT labeling and CLSM, although Nebelsick (1993) and Neuhaus (1994) describe the presence of nerves extending from the mouth cone ring to the pharynx. The special nature of this contractile epithelium may indicate the existence of another neurotransmitter that is different from serotonin and therefore, no pharyngeal-associated innervation was detected in this study. It is also possible that our methods for the labeling and detection of fine-scale pharyngeal innervation were not adequate.

Ventral longitudinal cord

High levels of anti-5-HT-like immunoreactivity were shown in the ventral nerve cord and large posterior somata of all species under investigation. The presence of a ventral ganglionated nerve cord in kinorhynchs was first recognized by Claparède (1863) and also reported on by subsequent authors (e.g., Zelinka, 1928; Kristensen and Higgins, 1991; Neuhaus and Higgins, 2002). Kristensen and Higgins (1991) identified a segmentally paired midventral chain of ganglia in *E. aquilonius* and *Pycnophyes greenlandicus* using TEM. Nebelsick (1993) added the presence of a caudal ganglion in her description of the nervous system of *E. capitatus*. These descriptions fit with the serotonin-like labeling of cells and neuropil characterized here in *E. spinifurca*. However, our results show four longitudinal strings in the anteriormost part of the ventral cord that transition to become three strings in segment 2 by the joining of the two central strings. These results are partially supported by those from *E. capitatus* (Nebelsick, 1993), in which the ventral cord has a double origin in the region of the introvert and becomes unpaired in the remaining trunk. These observations imply that the basic structure may be the same in both *E.*

*spinifurca* and *E. capitatus*, and that CLSM techniques enable a finer resolution than three-dimensional reconstruction from TEM transverse sections. The ventral nerve cord in *E. capitatus* arises from the anterior neuronal somata (when the introvert is withdrawn) and bends toward the ventral side to extend posteriorly toward the caudal end (Nebelsick, 1993). In our material, the ventral nerve cord appears to originate from either the posterior side of the anterior neuronal somata, or from the central neuropil; the exact position could not be determined precisely as double staining with propidium iodide and anti-5-HT antibodies was not performed. However, Kristensen and Higgins (1991) point to the posterior neuronal somata as the origin for the ventral cord. Our detection of two anterior, incomplete neuronal rings, that connect with the ventral nerve cord, and which may be associated with anterior neuronal somata, is more in line with Nebelsick' s observations.

No additional nerve cords along the body were labeled; however, this does not necessarily mean that such structures are absent. Our results do not reflect the orthogonal nervous system described previously with TEM showing eight additional longitudinal nerve cords connected with circular nerve fibers in each segment (Kristensen and Higgins 1991 in *E. aquilonius*; Nebelsick 1993 in *E. capitatus*). Twelve longitudinal nerve cords have been reported in *Zelinkaderes floridensis* (Neuhaus, 1994); only seven or eight longitudinal cords have been reported in the genus *Pycnophyes* (Kristensen and Higgins, 1991; Neuhaus, 1994). No information on the subject is known from the genus *Antygomonas*. It should also be noted that the available published information does not address the double, single or fused nature of the ventral nerve cords described in this study, with the exception of Nebelsick (1993) in *E. capitatus*, and illustrated by Neuhaus (1994) in *Z. floridensis* and *Pycnophyes dentatus*.

It cannot be excluded that a lack of signal in dorsal and lateral regions of the trunk segments is due to low levels of endogenous serotonin molecules or anti-5-HT antibodies. However, as stated above, serotonin may only appear in regions associated with muscular control implying that the remaining cords may have other functions, which could be primarily sensory. A midventral nerve cord has been previously described through TEM as innervating the segmental muscles and did not appear to have sensory function (Kristensen and Higgins, 1991), a statement in strong agreement with our results. Neuhaus (1994) and Neuhaus and Higgins (2002) described the neuromuscular junction through cell processes from muscle cells to elements of the nervous system. Our results from CLSM confirm this fact, because no neurites can be seen extending laterally from the ventral cord to the dorsoventral muscles. Further research that incorporates labeling for additional sensory neurotransmitters would be needed to confirm the functional role of the remaining longitudinal cords, and would also serve to clarify their structural relationships with different sensory organs (sensory spots) on the surface of the kinorhynch body.

Comparison within Kinorhyncha

The discussion above has revealed several variations among features of the nervous system in Kinorhyncha. The number of nerve strings in the ventral cord varies from four in *A. paulae* and *Z. brightae* to three in *E. spinifurca* by a joining of the two central neurites in the latter. While *E. spinifurca* shows an apparent ganglionated or segmental pattern of somata in every segment of the ventral nerve cord, they are sparsely scattered without a clear segmental pattern in *A. paulae* and *Z. brightae*. Because serotonin is hypothesized to be the primary myoexcitatory neurotransmitter, these differences may relate to the type and

arrangement of the trunk musculature, which is strongly segmented in *Echinoderes* (Kristensen and Higgins, 1991) and *Antygomonas* (Müller and Schmidt-Rhaesa 2003). The cuticle is distinctly thicker and more sclerotized in species of *Echinoderes* than it is in *Zelinkaderes* and *Antygomonas*. Functionally, the presence of a sclerotized cuticle in *E. spinifurca* agrees with its notable segmentation, which enables movements of an otherwise rigid trunk. This, in turn, involves the presence of strong, specific musculature that requires adequate attachment points (thick cuticle) and therefore is also arranged segmentally. Consequently, the innervation of this musculature may appear more condensed and segmentally specialized. Regarding their nervous system, homalorhagid kinorhynchs have been poorly studied (Schmidt-Rhaesa, 2007), although their thick sclerotized cuticle and segmented muscular system (Rothe and Schmidt-Rhaesa, 2004) generally support this line of reasoning.

Nebelsick (1993) described the ventral nerve cord terminating in a caudal ganglion in *E. capitatus*. In *E. spinifurca* there is a pair of big ventrolateral cell somata on segment 10 with strong serotonin-like IR, while in *A. paulae* and *Z. brightae* a conspicuous neurite loop occupies the last two segments. It is difficult to unequivocally correlate the two different structures reported here with the caudal ganglion of Nebelsick (1993). However, both functional and evolutionary implications can be suggested. The big ventrolateral somata and the neurite loop are located very close to the gonopores, suggesting a relationship with the control of muscles involved in reproduction. Due to cutting of the posterior end for immunolabeling in some of the studied specimens, it was not possible to identify them as males or females. Nevertheless, all of the specimens under investigation showed either the large posterior neural somata or the neurite loops described previously,

and therefore we assume that they exist in both sexes. Zelinka (1928) noted similar structures for *P. communis* and Higgins (1961) described that an enlarged posterior region of the double ventral nerve cord was present only in females. Kristensen and Higgins (1991) suggest the possibility that such structures have some special function, perhaps in secretory control for the deposition of eggs. Another possible function for these terminal structures related to reproduction in females could be to control the muscular contraction needed to squeeze the female seminal receptacles at the moment of fertilization. Regarding the presence of these neural structures in male individuals, it should be noted that the so-called penile spines are not connected with muscles, although their flexible structure is assumed to have a sensory function (Neuhaus, 1999; Neuhaus and Higgins, 2002). Therefore, in parallel with the role suggested above for females, these terminal nerve structures may be involved in the muscular control for the discharge of sperm. Thus far, specific muscles involved in this process in either males or females have not been described as part of the kinorhynch musculature (Müller and Schmidt-Rhaesa, 2003; Rothe and Schmidt-Rhaesa, 2004, Schmidt-Rhaesa and Rothe, 2006).

Alternatively, there is another function unrelated to reproduction that can be suggested. The ventrolateral large cell somata and loop could be involved in the muscular control of the highly movable terminal spines of kinorhynchs (laterotermínal spines, laterotermínal accessory spines and the midterminal spine). Each type of spine has strong musculature associated with it, at least in specimens of *Antygomonas* (Müller and Schmidt-Rhaesa, 2003). In this respect, it is very interesting that a terminal loop appears only in species having a midterminal spine, such as *A. paulae* and *Z. brightae*, while the paired lateroventral aggregations have been found only in species lacking a midterminal spine,

namely *E. spinifurca*. Juvenile stages of both Cyclorhagid and Homalorhagid species have a midterminal spine that does not remain in their respective adult stages. According to Neuhaus (1993), the possession of a midterminal spine during postembryonic development represents a plesiomorphic condition within Kinorhyncha. Therefore, the loss of a midterminal spine may have occurred independently during evolution in two unrelated families, Echinoderidae (Cyclorhagida) and Pycnophyidae (Homalorhagida). This hypothesis should be tested using a more comprehensive phylogenetic framework of relationships within the phylum.

Comparison with closely related groups

Kinorhyncha is most closely related to the groups Loricifera and Priapulida, which are often collectively referred to as Scalidophora (Lemburg, 1995). Kinorhyncha, Loricifera and Priapulida (only in Tubiluchidae) share a tripartite brain with anterior and posterior portions of neuronal somata separated by the centrally located neuropil, a feature that was likely inherited from their most recent common ancestor (Rothe and Schmidt-Rhaesa, 2010). A longitudinal arrangement of the brain somata into distinct radial clusters can also be recognized in close association with the first row of spines and introvert retractors: 10 lobes in Kinorhyncha, 8-10 in Loricifera and at least 8 in Priapulida (Kristensen and Higgins, 1991; Kristensen, 1991; Rothe and Schmidt-Rhaesa, 2010). With respect to the epidermis, the position of the brain lies terminally between the anteriormost ring of introvert appendages and the mouth cone (Nebelsick, 1993), and it is flanked by the introvert and mouth cone retractor muscles (Neuhaus, 1994; Nielsen, 2012), a position that is common among Kinorhyncha, Loricifera, and Priapulida. However, a detailed

examination suggests that the ring structure of the brain could be derived from a bilateral arrangement. The aggregation of anterior neuronal somata is not a complete ring but is horseshoe shaped, as advanced by Nebelsick (1993) and confirmed by our observations. It is clear that the circular or ring-like arrangement of the brain also corresponds to the circular pattern of introvert appendages or scalids, which show an arrangement of up to seven circles in variable numbers (Zelinka, 1928; Higgins, 1961; Kristensen and Higgins, 1991; Sørensen and Pardos, 2008). Such a circular arrangement does not exhibit a strict radial symmetry, but consistently shows elements suggesting an ancestral bilateral symmetry, particularly in the posteriormost rows or circles of scalids and trichoscalids. Environmental constraints from the intrabenthic, three-dimensional habitat of these animals may have lead to the development of this 'pseudo-radial' arrangement. Typically, bilateral elements of the introvert appendages are most clearly seen along the midventral line, a position corresponding to the point where the nerve rings of the brain are open or incomplete. Such bilateral elements are also present in other Scalidophorans, namely in the members of Loricifera, where specialized scalids constitute the so-called "double organ" (Kristensen, 1983; Higgins and Kristensen, 1986). And paired midventral scalids "break" the otherwise radial symmetry of the introvert in at least five genera and species of priapulids (Adrianov and Malakhov, 1999; Adrianov and Malakhov, 2001). Additional information on the brain structure of loriciferans (Kristensen 1991) and priapulids (Storch, 1991; Schmidt-Rhaesa, 2010) show a more complete, or perfect ring structure, suggesting that kinorhynchs represent the most plesiomorphic bilateral arrangement as far as the brain structure is concerned.

The presence of a partially or semi-paired ventral nerve cord in Kinorhyncha was previously reported by Nebelsick (1993) and our results for the genus *Echinoderes* agree with this statement. In priapulids, the ventral nerve cord is unpaired along its length while in loriciferans it is distinctly paired (Kristensen 1991). Rothe and Schmidt-Rhaesa (2010) assigned a derived apomorphic state for the unpaired ventral nerve cord of priapulids within Scalidophora, implying that a paired ventral nerve cord represents the plesiomorphic state. Regarding the segmental organization of the ventral nerve cord, loriciferans and most kinorhynchs show a ganglion-like clustered pattern, while priapulids do not show any such pattern. In priapulids and loriciferans, neuronal somata associated with the ventral nerve cord are scarce in the anteriormost trunk region, and may indicate an adaptation of the nervous system to mechanical stress associated with retraction and eversion of the introvert (Rothe and Schmidt-Rhaesa, 2010; Kristensen, 1991). Within kinorhynchs, this was previously reported for *E. capitatus* by Nebelsick (1993). We have not only confirmed this statement, but also show the precise location where four strings become three by the fusion of the two midventral strings within the first segment (see Results and Figs. 5, 6). This makes sense if, as suggested above, the location of fusion is where the ventral cord is firmly attached to the body wall. Anterior to this site, the cord is an apparently flexible bundle of neurites extending from the second incomplete ring that varies in position during introvert movements (Fig. 7).

The existence of a caudal ganglion has been previously reported in all scalidophorans: Loricifera (Kristensen, 1991; Malakhov and Adrianov 1995) Kinorhyncha (Kristensen and Higgins, 1991; Nebelsick, 1993) and Priapulida (Rothe and Schmidt-Rhaesa, 2010). We observed either anti-5-HT-like IR cell somata or a neurite loop within

segments 10-11, which are two distinct terminal structures. The presence of each structure is consistent between two well-defined kinorhynch groups with and without a midterminal spine, respectively, and the possible functional significance of each structure in relation to the process of reproduction and/or movement of the terminal spines has been discussed above. A posterior swelling of the ventral longitudinal nerve cord showing high anti-5-HT-like immunoreactivity has been reported at the base of the tail in several species of priapulids, and was considered to be the origin for innervation of the caudal appendage, which is absent in non-tailed priapulids (Rothe and Schmidt-Rhaesa, 2010). Similarly, we found a terminal neurite loop in species of kinorhynchs having a midterminal spine, while those species without such a spine also lack the terminal loop. Although a phylogenetic value has not been assessed for the priapulid tail, we hypothesize that the presence of a terminal neurite loop is a plesiomorphic feature within scalidophorans, and may be correlated with the occurrence of a terminal structure (midterminal spine, caudal appendage). To date, no immunolabeling data on the nervous system of loriciferans are available. Remarkably, loriciferan larvae have caudal appendages, the so-called toes that are absent in adults. A comparative study of caudal nerve structures in both larval and adult loriciferans is required in order to support or reject the plesiomorphic character status for a caudal nerve loop in Scalidophora.

Additional studies of the nervous system in these minor but relevant groups would help to clarify their internal and external phylogenetic relationships. Future investigations should extend the selection of molecular markers for neurotransmitters to obtain a more comprehensive picture of nervous system architecture in Kinorhyncha.

## ACKNOWLEGDEMENTS

We are grateful for the assistance of Dr. Mary Rice and Dr. Jon Norenburg, who acted as scientific advisors to M. Herranz. Dr. Valerie Paul (Head Scientist) and the staff of the Smithsonian Marine Station at Fort Pierce (SMSFP) provided us with excellent working facilities and technical support. Dr. Rick Hochberg, Lowell University, MA, generously provided some of the fluorochrome reagents. This work has been conducted with financial support from a Link Foundation/Smithsonian Institution Graduate Fellowship to M. Herranz, and from the Ministerio de Ciencia y Tecnología, Plan Nacional de Investigación Científica, Desarrollo e Investigación Tecnológica (CGL2009-08928) to F. Pardos. This publication is Smithsonian Marine Station contribution No.XXXX

## REFERENCES

Adrianov AV, Malakhov VV. 1999. Cephalorhyncha of the World Ocean. Moscow: KMK Scientific Press. p 1-400.

Adrianov AV, Malakhov VV. 2001. Symmetry of priapulids (Priapulida). J Morphol 247: 99-121.

Ahlrichs W. 1995. Ultrastruktur und Phylogenie von *Seison nebaliae* (Grube 1859) und *Seison annulatus* (Claus 1876). Hypothesen zu phylogenetischen Verwandtschaftsverhältnissen innerhalb der Bilateria. Göttingen, Germany: Cuvillier Verlag.

583 Brown R. 1989. Morphology and ultrastructure of the sensory appendages of a kinorhynch
584 introvert. Zool Scr 18:471-182.

585 Brown R, Higgins RP. 1983. A new species of *Kinorhynchus* (Homalorhagida,
586 Pycnophyidae) from Australia with a redescription and range extension of other
587 Kinorhyncha from the South Pacific. Zool Scr 12:161-169.

588 Brenneis G, Richter S. 2010. Architecture of the nervous system in Mystacocarida
589 (Arthropoda, Crustacea) an immunohistochemical study and 3D reconstruction. J Morphol
590 271:169-189.

591 Budd GE, Telford MJ. 2009. The origin and evolution of arthropods. Nature 457:812-817.

592 Bullock TH, Horridge GA. 1965. Structure and Function in the Nervous Systems
593 of Invertebrates. San Francisco: W.H. Freeman. 1179 p.

594 Claparède E. 1863. Beobachtungen über die Anatomie und Entwicklungsgeschichte
595 wirbelloser Thiere an der Küste der Normandie angestellt. Leibzig: Wilhelm Engelmann.

596 Dunn CW, Hejnol A, Matus DQ, Pang K, Browne WE, Smith SA, Seaver E, Rouse GW,
597 Obst M, Edgecombe GD, Sørensen MV, Haddock SHD, Schmidt-Rhaesa A, Okusu A,
598 Møbjerg Kristensen R, Wheeler WC, Martindale MQ, Giribet G. 2008. Broad
599 phylogenomic sampling improves resolution of the animal tree of life. Nature 452:745-749.

600 Edgecombe GD, Giribet G, Dunn CW, Hejnol A, Kristensen RM, Neves RC, Rouse GW,
601 Worsaae K, Sørensen MV. 2011. Higher-level metazoan relationships: recent progress and
602 remaining questions. Org Divers Evol 11:151–172.

Gª Ordóñez D, Pardos F, Benito J. 2000. Cuticular structures and epidermal glands of *Echinoderes cantabricus* and *E. hispanicus* (Kinorhyncha, Cyclorhagida) with special reference to their taxonomic value. J Morphol 246:161-178.

Garey JR. 2001. Ecdysozoa: The relationship between Cycloneuralia and Panarthropoda. Zool Anz 240: 321-330.

Hejnol A, Obst M, Stamatakis A, Ott M, Rouse GW, Edgecombe GD, et al. (2009). Assessing the root of bilaterian animals with scalable phylogenomic methods. Proc R Soc Biol Sci 476:4261-4270.

Higgins RP. 1961. Morphological, larval, and systematic studies of the Kinorhyncha. Ph.D. Thesis, Duke University. 1-262.

Higgins RP. 1988. Kinorhyncha. In: Higgins RP, Thiel H (eds) Introduction to the study of Meiofauna. Washington DC: Smithsonian Institution Press. p 328-33.

Higgins RP. 1990. Zelinkaderidae, a new family of cyclorhagid Kinorhyncha. Smithson Contr Zool 500:1-26.

Higgins RP, Kristensen RM. 1986. New Loricifera from southeastern United States coastal waters. Smithson Contr Zool 438: 1-70.

Higgins RP, Kristensen RM. 1988. Kinorhyncha from Disko Island, West Greenland. Smithson Contrib Zool 458:1-56.

Hochberg R. 2007. Comparative immunohistochemistry of the cerebral ganglion in Gastrotricha: ananalysis of FMRFamide-like immunoreactivity in *Neodasys cirritus*

(Chaetonotida), *Xenodasys riedli* and *Turbanella* cf. *hyalina* (Macrodasyida). Zoomorphology 126:245-264.

Hochberg R. 2009. Serotonergic and SCPb-like innervation of the atrial complex in *Gyratrix hermaphroditus* (Platyhelminthes, Kalyptorhynchia) revealed with CLSM. Zoomorphology 128:169-181.

Hochberg R, Atherton S. 2011. A new species of *Lepidodasys* (Gastrotricha, Macrodasyida) from Panama with a description of its peptidergic nervous system using CLSM, anti-FMRFamide and anti-SCPB. Zool Anz 250:111-222.

Hochberg R, Gurbuz O. 2008. Comparative morphology of the somatic musculature in species of *Hexarthra* and *Polyarthra* (Rotifera, Monogononta): Its function in appendage movement and escape behavior. Zool Anz 247:233-248.

Kristensen RM. 1983. Loricifera, a new phylum with aschelminthes characters from meiobenthos. Z zool Syst Evolut 21:163-180.

Kristensen R M. 1991. Loricifera. In: F. W. Harrison and E. E. Ruppert. Microscopic anatomy of invertebrates, Vol. 4, Aschelminthes. New York: Wiley-Liss. p 351-375.

Kristensen R M, A Hay-Schmidt. 1989. The protonephridia of the Arctic kinorhynch *Echinoderes aquilonius* (Cyclorhagida, Echinoderidae). Acta Zool 70:13 27.

Kristensen RM, Higgins RP. 1991. Kinorhyncha. In: FW Harrison, and EE Ruppert. Microscopic anatomy of invertebrates, vol 4, Aschelminthes. New York: Wiley-Liss. p 377-404.

Lemburg C. 1995. Ultrastructure of sense organs and receptor cells of the neck and lorica of the *Halicryptus spinulosus* larva (Priapulida). Microfauna Marina 10:7-30.

Malakhov VV, Adrianov AV. 1995. Cephalorhyncha - A new phylum of the animal kingdom. Moscow: KMK Scientific Press. p 1-199.

Merriman JA, Corwin HO. 1973. An electron microscopical examination of *Echinoderes dujardini* Claparède (Kinorrhyncha) (sic). Z Morph Okol Tiere 76:227-242.

Moritz K, Storch R. 1972a. Zur Feinstruktur des Integuments von *Trachydemus giganteus* Zelinka .Kinorhyncha). Z Morph Okol Tiere 71:189-202.

Moritz K, Storch V. 1972b. Uber den ultrastrukturellen Bau der Skaliden von *Trachydemus giganteus* (Kinorhyncha). Mar Biol 16:81-89.

Nebelsick M. 1993. Introvert, mouth cone, and nervous system of *Echinoderes capitatus* (Kinorhyncha, Cyclorhagida) and implications for the phylogenetic relationships of Kinorhyncha. Zoomorphology 113:211-232.

Neuhaus B. 1994. Ultrastructure of alimentary canal and body cavity, ground pattern, and phylogenetic relationships of the Kinorhyncha. Microfauna Marina 9:61-156.

Neuhaus B. 1999. Kinorhyncha. In: Knobil E, Neill JD (Hrsg) Encyclopedia of Reproduction. Vol 2 Academic Press, San Diego. p 933-937.

Neuhaus B, Higgins R P. 2002. Ultrastructure, biology and phylogenetic relationships of Kinorhyncha. Integ Comp Biol 42:619-632.

Nielsen C.1995. Animal evolution. Interrelationships of the living phyla. 1st Edn. Oxford, UK: Oxford University Press.

Nielsen C. 2012. Animal evolution. Interrelationships of the living phyla. 3rd Edn. Oxford, UK: Oxford University Press. 578 p.

Müller M, Schmidt-Rhaesa A. 2003. Reconstruction of the muscle system in *Antygomonas* sp. (Kinorhyncha, Cyclorhagida) by means of phalloidin labeling and CLSM. J Morphol 256:103-110.

Pardos F, Higgins RP, Benito J. 1998. Two new *Echinoderes* (Kinorhyncha, Cyclorhagida) from Spain, including a reevaluation of Kinorhynch taxonomic characters. Zool Anz 237:195-208.

Richter S, Loesel R, Purschke G, Schmidt-Rhaesa A, Scholtz G, Stach T, Vogt L, Wanninger A, Brenneis G, Döring C, Faller S, Fritsch M, Grobe P, Heuer CM, Kaul S, Møller OS, Müller CHG, Rieger V, Rothe BH, Stegner MEJ, Harzsch S. 2010. Invertebrate neurophylogeny: suggested terms and definitions for a neuroanatomical glossary. Front Zool, 7:29. doi:10.1186/1742-9994-7-29.

Rothe B, Schmidt-Rhaesa A. 2004. Probable development from continuous to segmental longitudinal musculature in *Pycnophyes kielensis* (Kinorhyncha, Homalorhagida). Meiofauna Mar 13:21-28.

Rothe B, Schmidt-Rhaesa A. 2009. Architecture of the nervous system in two *Dactylopodola* species (Gastrotricha, Macrodasyida). Zoomorphology 128:227-246.

Rothe B, Schmidt-Rhaesa A. 2010. The structure of the nervous system in *Tubiluchus troglodytes* (Priapulida). Invertebr Biol 129(1):39-58.

Schmidt-Rhaesa A. 1998. Phylogenetic relationships of the Nematomorpha- a discussion of current hypothesis. Zool Anz 236: 203-216.

Schmidt-Rhaesa A. 2007. The evolution of organ systems. New York: Oxford University Press Inc. p 104-105.

Schmidt-Rhaesa A, Rothe B. 2006. Postembryonic development of dorsoventral and longitudinal musculature in *Pycnophyes kielensis* (Kinorhyncha, Homalorhagida). Integr Comp Biol 46:144-150.

Sørensen MV, Heiner I, Ziemer O. 2005. A new species of *Echinoderes* from Florida (Kinorhyncha: Cyclorhagida). Proc Biol Soc Wash 118:499-508.

Sørensen MV. 2007. A new species of *Antygomonas* (Kinorhyncha: Cyclorhagida) from the Atlantic coast of Florida, USA. Cah Biol Mar 48:155-168.

Sørensen MV, Pardos F. 2008. Kinorhynch systematics and biology an introduction to the study of kinorhynchs, inclusive identification keys to the genera. Meiofauna Mar 16:21-73.

Sørensen MV, Hebsgaard MB, Heiner I, Glenner H, Willerslev E, Kristensen RM. 2008. New data from an enigmatic phylum: evidence from molecular sequence data supports a sister-group relationship between Loricifera and Nematomorpha. J Zool Eyst Evol Res 46:231-239.

Storch V. 1991. Priapulida. In: FW Harrison, EE Ruppert. Microscopic anatomy of invertebrates, vol 4, Aschelminthes. New York: Wiley-Liss. p. 377-404.

Telford MJ, Bourlat SJ, Economou A, Papillon D, Rota- Stabelli O. 2008. The evolution of the Ecdysozoa. Phil Trans R Soc B 363:1529-1537.

Worsaae K, Rouse GW. 2010. The simplicity of males: dwarf males of four species of *Osedax* (Siboglinidae; Annelida) investigated by Confocal Laser Scanning Microscopy. J Morphol 271:127-142.

Zelinka C. 1928. Monographie der Echinodera. Leipzig: Verlag Wilhelm Engelmann.

**Figure captions**

**Fig. 1** Scanning electron micrographs of the external anatomy of three cyclorhagid kinorhynch species. **A** *Echinoderes spinifurca* in ventrolateral view with anterior to the right and introvert extended; **B** *Antygomonas paulae* in lateral view of with anterior to the top right and introvert extended; **C** *Zelinkaderes brightae* in ventral view with anterior to the top and introvert retracted. acs, acicular spine; cus, cuspidate spine; I, introvert; lts, laterotermínal spine; mc, mouth cone; mds, middorsal spine; mts, midterminal spine; sc, scalid; s1, segment one; s11, segment eleven; te, tergal extension.

**Fig. S-1** Confocal laser scanning micrographs of the external anatomy of three cyclorhagid kinorhynch species. Cuticular structures are autofluorescent when exposed to an excitation wavelength of 488 nm. All specimens are oriented with anterior to the top. The images are confocal z-stack projections. **A, D** *Echinoderes spinifurca* in ventral and lateral views,

721 respectively; **B, C** *Antygomonas paulae* in ventral and dorsal views; **E, F** *Zelinkaderes*
722 *brightae* in ventral and dorsal views. Scale bars: 50 µm. acs, acicular spine; cus, cuspidate
723 spine; go, gonopore; I, introvert; ltas, laterotermінal accessory spine; lts, laterotermінal
724 spine; mc, mouth cone; mds, middorsal spine; mts, midterminal spine; ne, neck; sc, scalid;
725 s1, segment one; s11, segment eleven; ss, sensory spot; te, tergal extension.

726 **Fig. 2** Propidium iodide labeling of DNA in *Echinoderes spinifurca*. The images are
727 confocal z-stack projections. **A** ventral view of a male specimen with anterior to the top; **B**
728 – **E** optical cross sections through different brain regions corresponding to the dotted lines
729 indicated with B, C, D and E in image **A**; each cross section is orientated with ventral side
730 to the bottom. Dashed circles in B and C indicate distinct clusters of cell nuclei in the
731 anterior neural somata. Visible scalids and segmented cuticle outlines are autofluorescent.
732 Testes (t) are identified as long internal sacs filled with elongate, wavy nuclei within
733 segments 4–10 flanking the gut. Scale bars: 20 µm. ans, anterior neuronal somata; br, brain;
734 cn, central neuropil; ipe, internal pharynx epithelium; mcnr, mouth cone nerve ring; pns,
735 posterior neuronal somata; t, testes; vlcc, ventrolateral cell cluster; vnc ventral nerve cord.

736 **Fig. 3** Propidium iodide labeling of DNA in *Antygomonas paulae.* The images are confocal
737 z-stack projections. **A** ventral view of an adult female with anterior to the top; the brain is
738 regionally divided into two neural somata aggregations separated by a central neuropil.
739 Female seminal receptacles appear as posterior sacs filled with elongate nuclei; **B** – **D**
740 optical cross sections through different brain regions corresponding to the dotted lines
741 indicated with B, C, and D in image **A**; each cross section is orientated with ventral side to
742 the bottom. Visible scalids, spines and segmented cuticle outlines are autofluorescent. Scale

bars: 20 μm. ans, anterior neuronal somata; br, brain; cn, central neuropil; ph, pharynx; pns, posterior neuronal somata; rs, receptaculum seminis; vnc, ventral nerve cord.

**Fig. 4** Comparison of Propidium iodide labeling and serotonin-like immunoreactivity in the central nervous system of *Echinoderes spinifurca*. Each specimen is oriented in ventral view with anterior to the top. **A** confocal z-stack projection of cell nuclei in the brain and ventral nerve cord; **B** confocal z-stack projection of serotonergic-like elements in the brain and ventral nerve cord. Dashed horizontal lines separate the five anterior segments from the four posteriormost segments (s8 - s11) in each specimen; central segments regions are not shown. Variation in the position of brain structures between specimens A and B is the result of independent retraction of introvert and mouth cone musculature. The positions of posterior ventral nerve cord structures in A and B are similar. Visible scalids and body segment divisions are autofluorescent. Scale bars: 20 μm. ans, anterior neuronal somata; br, brain; cn, central neuropil; cne, convergent neurite; $inr_1$, first incomplete ring; $inr_2$, second incomplete ring; mcnr, mouth cone nerve ring; ph, pharynx; pns, posterior neuronal somata; s, segment; t, testes; vlcc, ventrolateral cell cluster; vls, ventrolateral somata; vms, ventromedial somata; vnc, ventral nerve cord; numbers in parentheses indicate the number of detectable vnc neurites at those locations, an asterisk marks the posterior end of the central neurite in the vnc.

**Fig. 5** Schematic drawing of serotonin-like immunoreactive elements in the central nervous system of *Echinoderes spinifurca*. **A** ventrolateral view of an adult with anterior to the top; both the introvert and mouth cone are extended; **B** enlarged view of the anterior ventral nerve cord showing the transition of 4 neurite strings into 3 neurite strings. bne, basket

neurite; cne, convergent neurites; g, gut; inr, incomplete rings; mcnr, mouth cone nerve ring; nc, nerve cluster; nr, nerve rings; vls, ventrolateral somata; vms, ventromedial somata; vnc, ventral nerve cord; vps, ventral paired somata.

**Fig. 6** Positional comparisons of serotonin-like immunoreactive elements in the central nervous system of *Echinoderes spinifurca*. The images are confocal z-stack projections. **A** lateral view with anterior to the top; when the introvert is retracted, the mouth cone nerve ring (mcnr) is anterior to the incomplete nerve rings ($inr_{1, 2}$); **B** – **D** ventral views showing the position of anterior 5-HT-like IR elements relative to changes in the amount of introvert extension; anterior is to the top. The position of the ring complex (arrows) relocates during extension and retraction of the introvert; **E** dorsal view showing relative positions of several anterior 5-HT-like IR elements. The anterior end of the ventral nerve cord is attached to the body within the first segment (dashed circles) and does not relocate during extension and retraction of the introvert. Distinct groups of neuronal cell bodies (arrowheads) are present in each segment along the vnc. Visible scalids and body segment divisions are autofluorescent. Scale bars: 20 µm. an asterisk marks the posterior end of the central neurite in the vnc. bne, basket neurite; $inr_{1,}$ first incomplete ring; $inr_{2,}$ second incomplete ring; mcnr, mouth cone nerve ring; vms, ventromedial somata; vnc, ventral nerve cord.

**Fig. 7** Schematic drawing of serotonin-like immunoreactive elements in the anterior central nervous system of *Echinoderes spinifurca*. **A** lateral view with ventral side down and anterior to the left; introvert is extended. **B** lateral view with ventral side is down and anterior to the left; introvert is retracted. The ring complex (rc) and convergent neurites

(cne) relocate in association with introvert movements, while the ventral nerve cord remains attached at the first fixed somata (ffs). The central neuropil is not shown relative to the position of anterior incomplete rings and posterior rings. Dashed lines indicate the location of basket neurites, which typically exhibit lower levels of immunoreactivity. bne, basket neurite; ffs, first fixed somata of the ventral nerve cord; cne, convergent neurite; $inr_{1,}$ first incomplete ring; $inr_{2,}$ second incomplete ring; mcnr, mouth cone nerve ring; $nr_{3,4,}$ nerve rings 3 and 4; rc, ring complex; s, soma; vms, ventromedial somata; vnc, ventral nerve cord; vps, ventral paired somata.

**Fig. 8** Serotonin-like immunoreactivity in the central nervous system of *Antygomonas paulae.* The images are confocal z-stack projections. **A** lateral view with anterior to the top; introvert is retracted; **B** ventral view of segments 1-8 with anterior to the top; introvert is retracted; **c** ventral view of posterior segments 7-11; the terminal loop of the vnc extends between segments 10-11. An asterisk marks the posterior end of the central neurite in the vnc. Numbers in parentheses indicate the number of detectable vnc neurites at those locations. Visible scalids, spines and body segment divisions are autofluorescent. Scale bars: 50 µm. cne, convergent neurite; $inr_{1,}$ first incomplete ring; $inr_{2,}$ second incomplete ring; lts, laterolateral spine; mcnr, mouth cone nerve ring; mls, midlateral somata; mts, midterminal spine; $nr_{3,4,}$ nerve rings 3 and 4; rc, ring complex; tl, terminal loop; vms, ventromedial somata; vnc, ventral nerve cord.

**Fig. 9** Serotonin-like immunoreactivity in the central nervous system of *Zelinkaderes brightae.* The images are confocal z-stack projections. **A** ventral view with anterior to the top; the introvert is retracted and the posterior region of segment 11 has been removed; **B**

ventral view of the posterior segments (s9, s10, s11) with anterior to the top; the terminal loop of the vnc extends between segments 10 and 11, and appears to be damaged on the right side. An asterisk marks the posterior end of the central neurite in the vnc. Numbers in parentheses indicate the number of detectable vnc neurites at those locations. Visible scalids, spines and body segment divisions are autofluorescent. Scale bars: 50 µm. cne, convergent neurite; $inr_{1,}$ first incomplete ring; $inr_{2,}$ second incomplete ring; lts, lateral terminal spine; mcnr, mouth cone nerve ring; mls, midlateral somata; mts, midterminal spine; $nr_{3, 4,}$ nerve rings 3 and 4; rc, ring complex; tl, terminal loop; vms, ventromedial somata; vnc, ventral nerve cord.

**Fig. 10** Schematic drawing of comparative serotonin-like immunoreactivity in the anterior central nervous system of three cyclorhagid kinorhynch species. **A** *Zelinkaderes* brightae; **B** Antygomonas *paulae*; **C** *Echinoderes spinifurca*. Ventral views with anterior to the top. Compared with *E. spinifurca*, the depth of introvert and mouth cone retraction within *Z. brightae* and *A. paulae* is greater (gray lines), which relocates the mouth cone nerve ring (mcnr) to the posterior end of the ring complex. The number of neurites in the ventral nerve cord is also different between *E. spinifurca* and the other two species. Dashed lines represent the presence of the basket neurites. bne, basket neurite; cne, convergent neurite; $inr_{1,}$ first incomplete ring; $inr_{2,}$ second incomplete ring; mcnr, mouth cone nerve ring; mls, midlateral somata; $nr_{3, 4,}$ nerve rings 3 and 4; rc, ring complex; vms, ventromedial somata; vnc, ventral nerve cord; vpg, ventral paired somata.

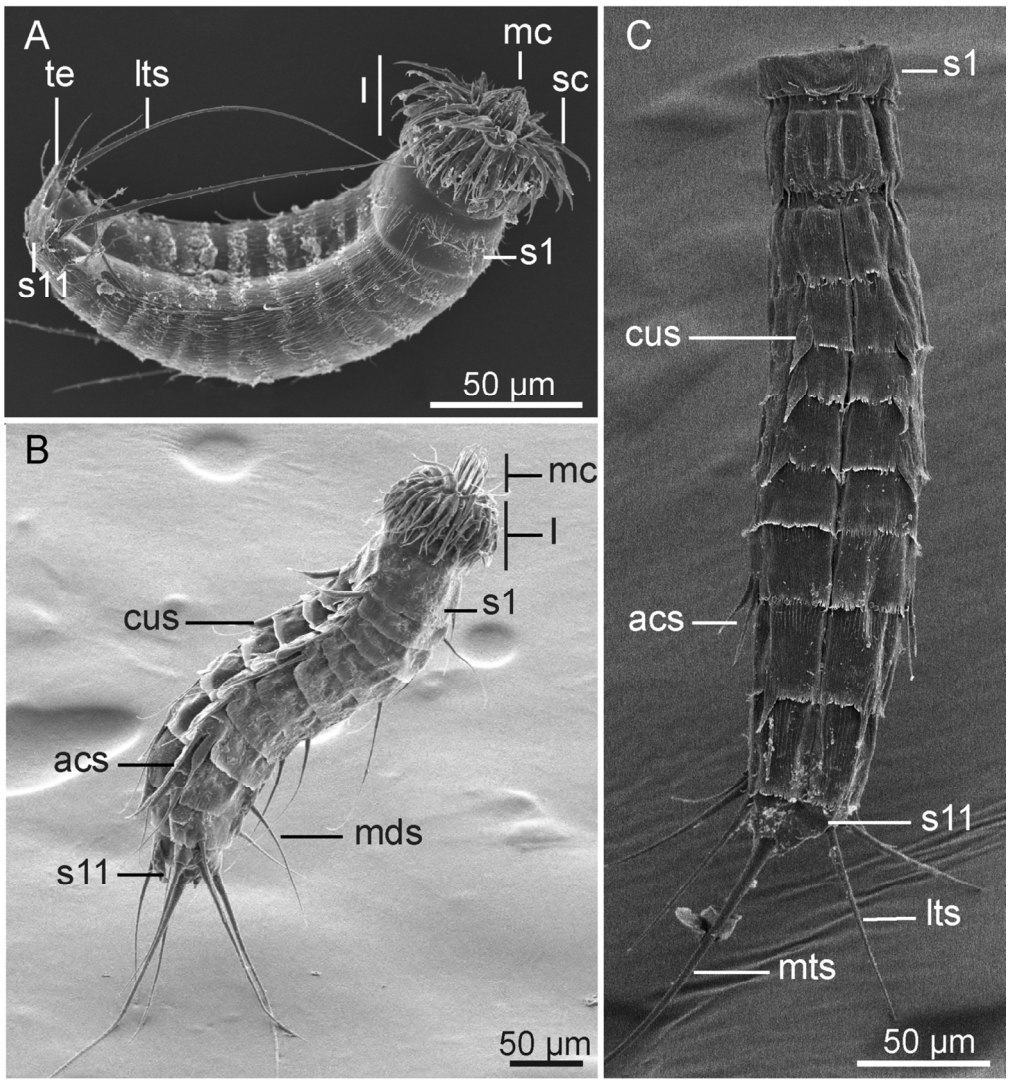


125x134mm (300 x 300 DPI)

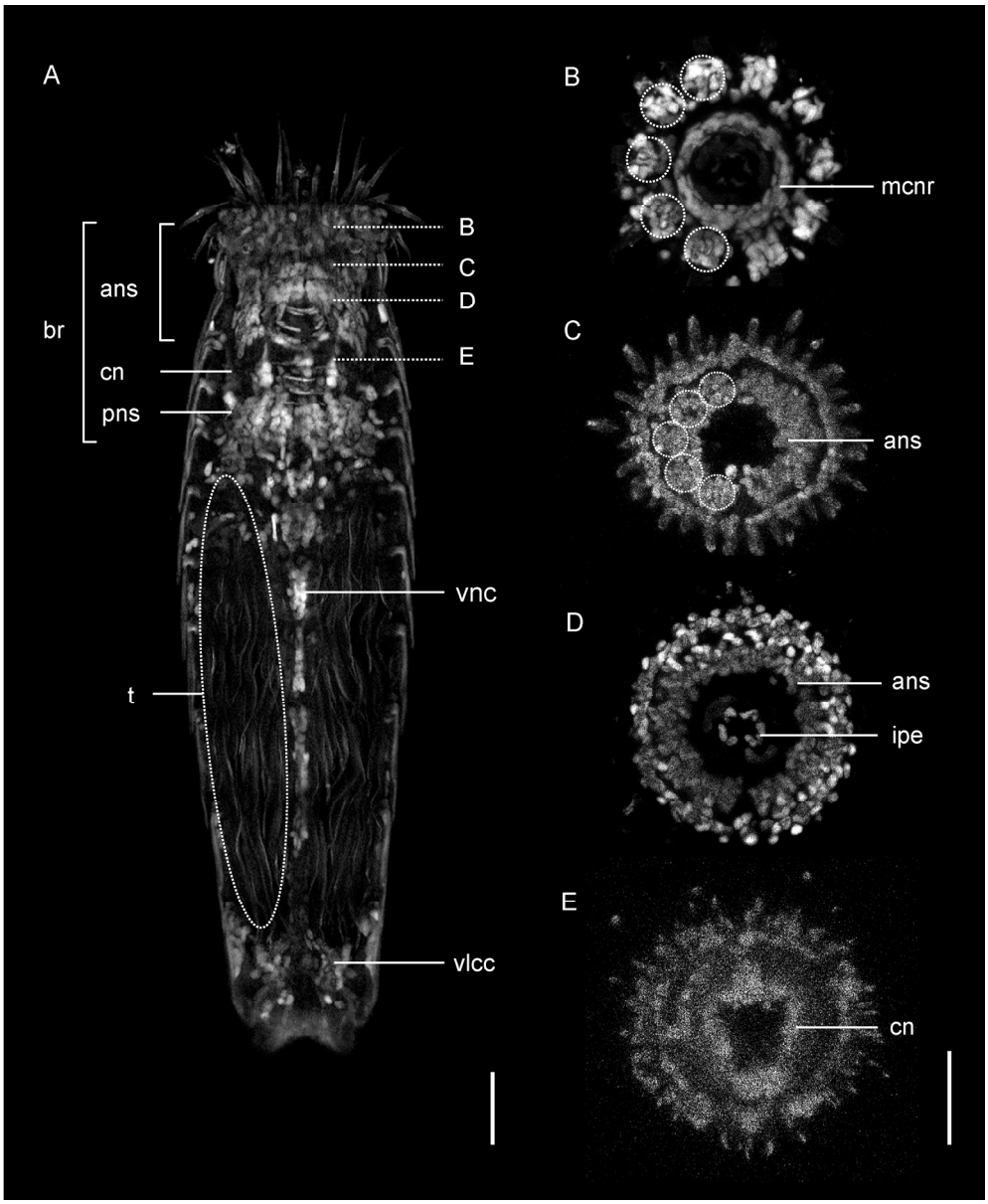


211x256mm (300 x 300 DPI)

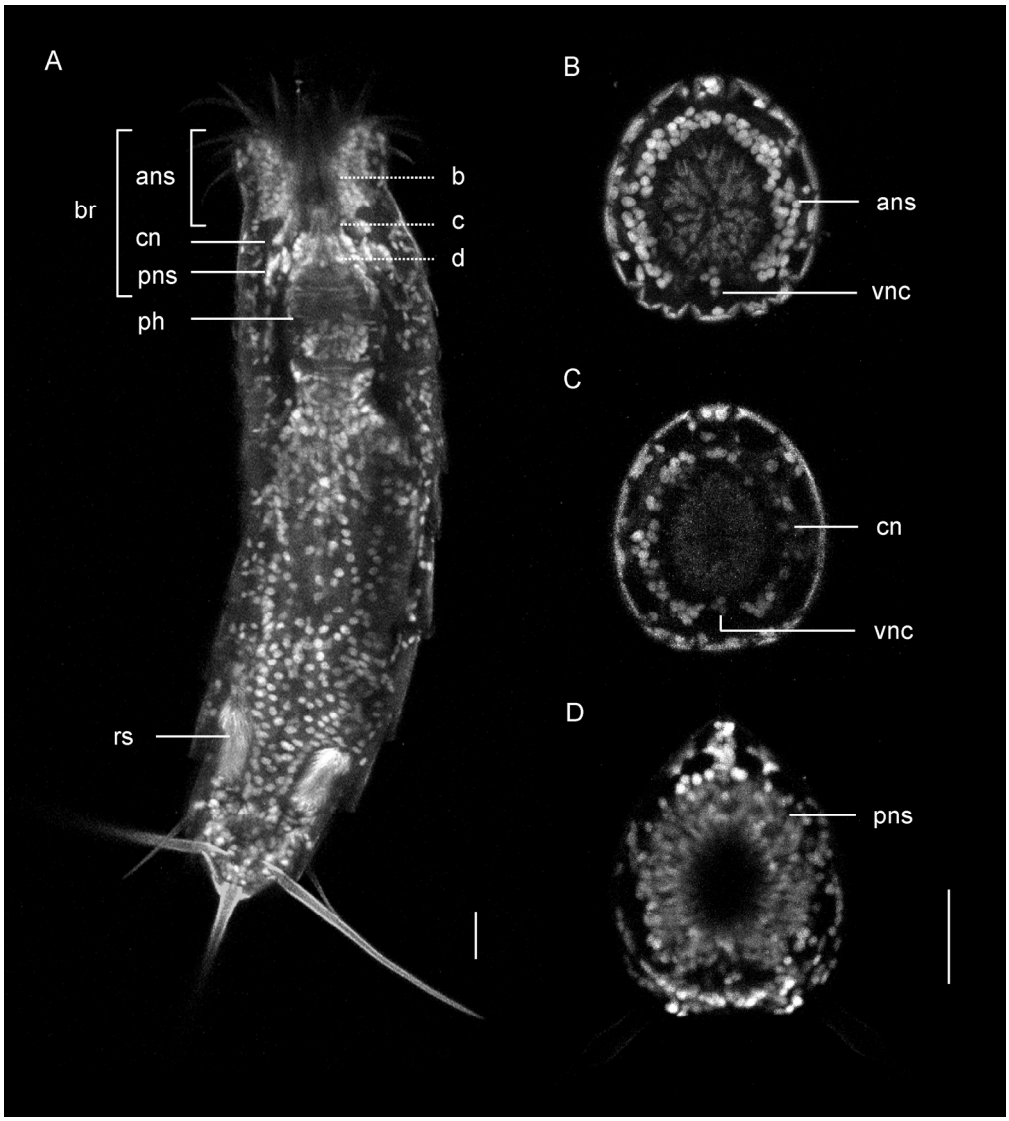


189x209mm (300 x 300 DPI)

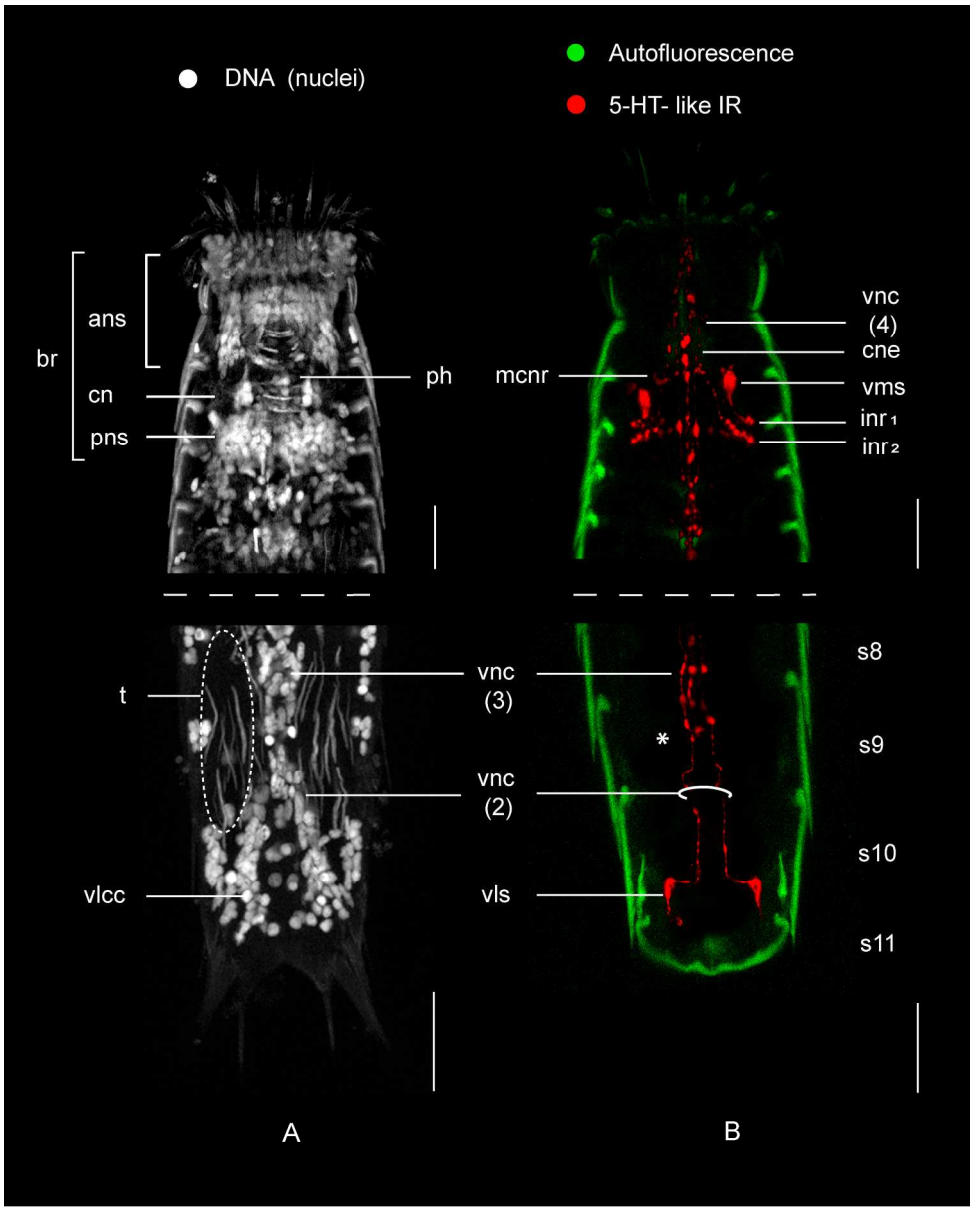


211x263mm (300 x 300 DPI)

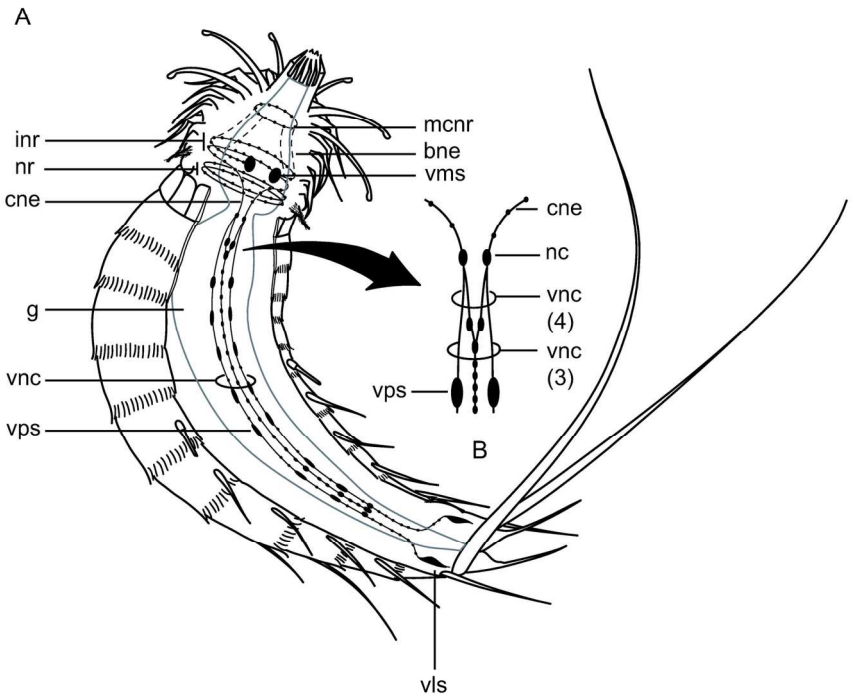


159x134mm (300 x 300 DPI)

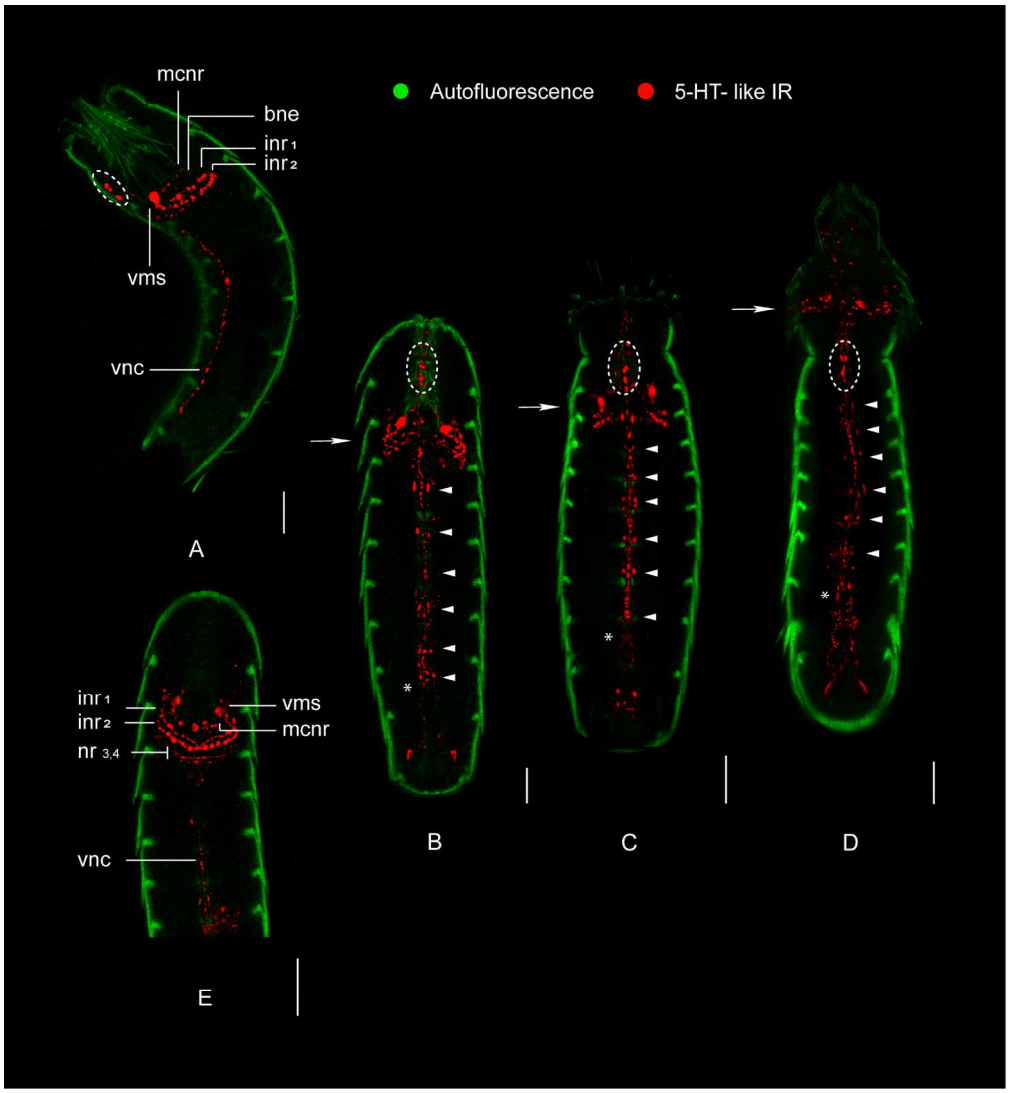


186x201mm (300 x 300 DPI)

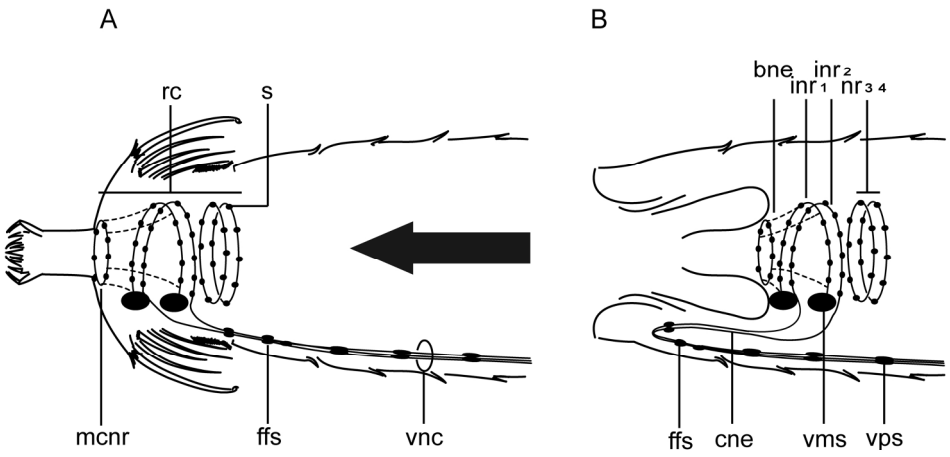


99x57mm (600 x 600 DPI)

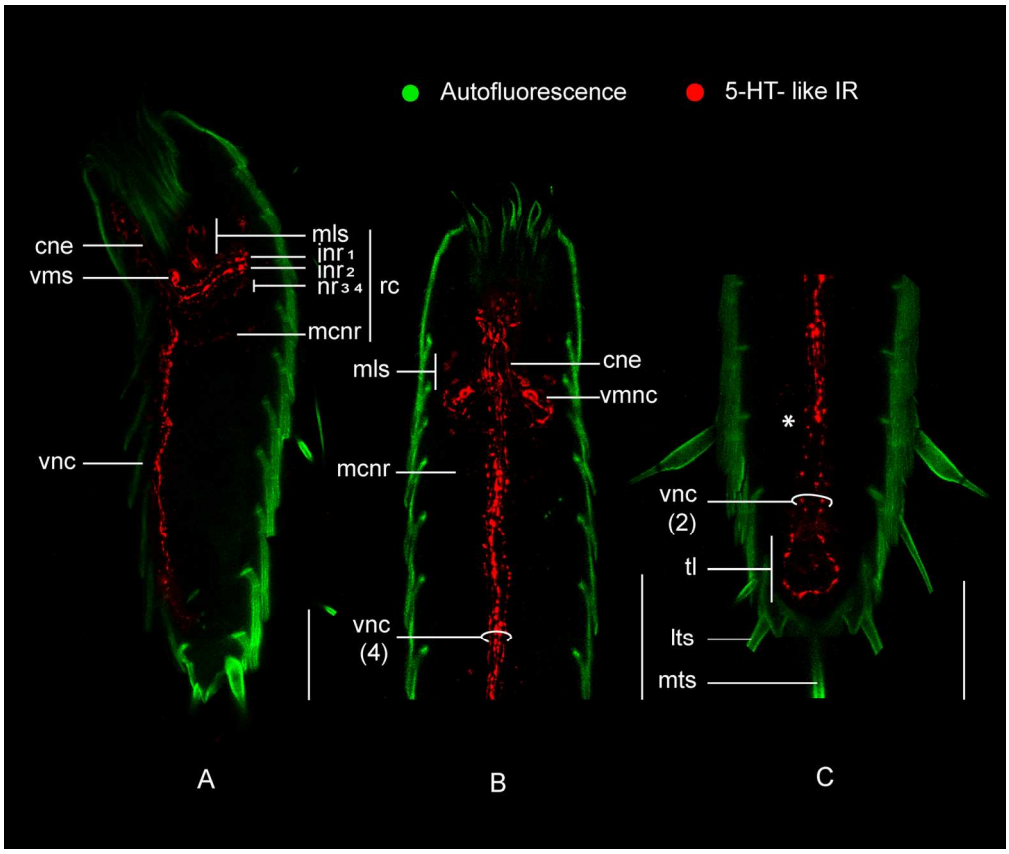


147x124mm (300 x 300 DPI)

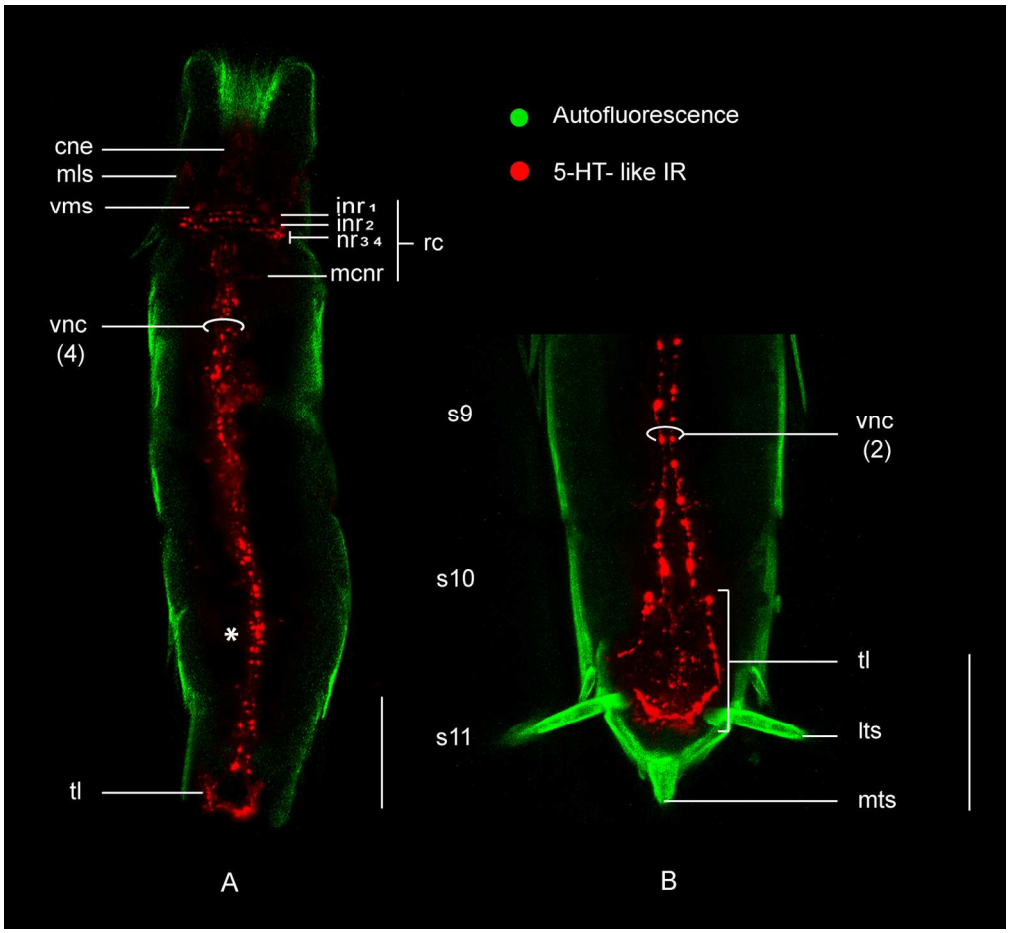


162x149mm (300 x 300 DPI)

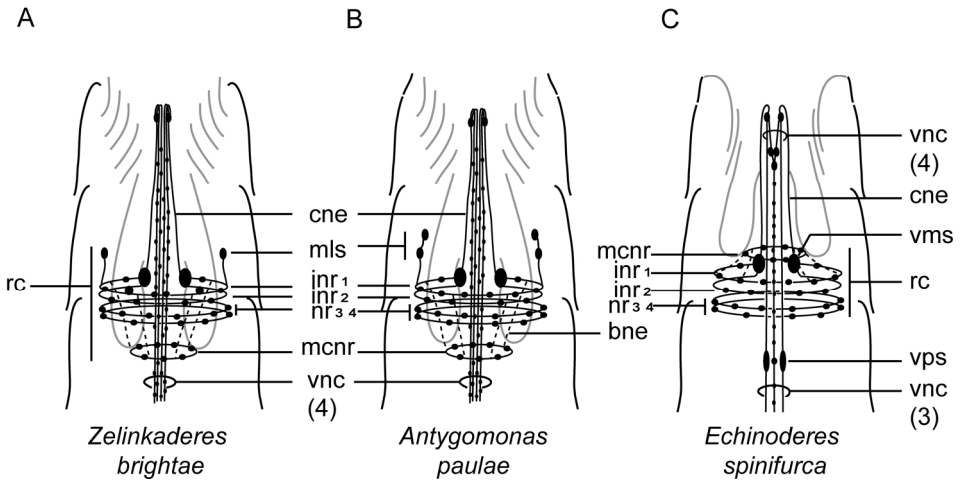


93x50mm (600 x 600 DPI)